

# PARP-1 inhibition sensitizes temozolomide-treated glioblastoma cell lines and decreases drug resistance independent of MGMT activity and *PTEN* proficiency

ANA P. MONTALDI<sup>1</sup>, SARAH C.G. LIMA<sup>1</sup>, PAULO R.D.V. GODOY<sup>1</sup>,  
DANILO J. XAVIER<sup>1</sup> and ELZA T. SAKAMOTO-HOJO<sup>1,2</sup>

<sup>1</sup>Department of Biology, Faculty of Philosophy, Sciences and Letters at Ribeirão Preto, University of São Paulo (USP), Ribeirão Preto, São Paulo 14040-901; <sup>2</sup>Department of Genetics, Ribeirão Preto Medical School, University of São Paulo (USP), Ribeirão Preto, São Paulo 14049-900, Brazil

Received January 30, 2019; Accepted March 22, 2020

DOI: 10.3892/or.2020.7756

**Abstract.** Information on the mechanisms that are associated with tumor resistance has the potential to provide the fundamental basis for novel therapeutic strategies. In glioblastoma (GBM), predictive biomarkers of cellular responses to temozolomide (TMZ) combined with poly-ADP-ribose polymerase inhibitor (PARPi) remain largely unidentified. In this context, the influence of MGMT (O<sup>6</sup>-methylguanine DNA methyltransferase) and *PTEN* (phosphatase and tensin homologue deleted on chromosome ten) has been studied in addition to the occurrence of synthetic lethality involving *PTEN* and PARPi. The present study investigated whether PARP-1 inhibition by NU1025 may increase the cytotoxicity of TMZ-induced lesions in GBM cells, and whether these mechanisms can be influenced by MGMT and *PTEN* status. The impact of *PTEN* deficiency in repair pathways, and the effects of PARP-1 inhibition and *PTEN* silencing, in terms of synthetic lethality, were also assessed. NU1025 combined with TMZ effectively sensitized TMZ-resistant cells (T98G *PTEN*-mutated and LN18 *PTEN*-wild-type) and TMZ-sensitive cells (U251MG *PTEN*-mutated), in contrast to NU1025 alone. However, the sensitizing effects were not observed in U87MG (*PTEN*-mutated) cells, suggesting that specific genetic alterations may influence the response to drug treatment. The sensitizing effects occurred independently of MGMT activity, which was evaluated in O6-BG-treated cells. *PTEN* silencing using small interfering (si)RNA did not sensitize *PTEN*-proficient cells to TMZ + NU1025, or

NU1025 alone, indicating an absence of synthetic lethality. The responses to TMZ + NU1025 involved antiproliferative activity, G2/M arrest, double strand breaks and the induction of apoptosis. Following 20 days of recovery after three consecutive days of TMZ treatment, TMZ-resistant cells were observed. However, when TMZ was combined with NU1025, the viability of T98G and LN18 cells was extremely decreased, indicating a lethal drug combination. Therefore, independently of MGMT proficiency and *PTEN* status, TMZ combined with PARPi may be a promising strategy that can be used to overcome TMZ acquired resistance in GBM cells.

## Introduction

Glioblastoma (GBM) is the most common and highly malignant glial tumor (Grade IV - World Health Organization). Complete surgical resection and adjuvant treatments (chemotherapy and radiotherapy) improve patient survival, but the prognosis for adult patients with GBM remains poor, with a median survival of 15-18 months (1-3). Temozolomide (TMZ) has been the most widely used drug treatment for patients with GBM (4), and *MGMT* promoter methylation has been considered to be a predictor for chemotherapeutic response to alkylating and methylating agents (5,6). However, there is a possibility that other DNA repair pathways may also promote GBM resistance to TMZ-induced base lesions (7). N<sup>7</sup>-methyl-guanine (N7-methyl-G) and N<sup>3</sup>-methyl-adenine (N3-methyl-A) adducts comprise >80% of TMZ-induced DNA lesions and are processed through base excision repair (BER), which is a multi-protein mechanism that is initiated by several damage-specific glycosylases (8). Therefore, resistance to TMZ can be caused by an efficient repair process via BER (9-11), although other alternative processes may also occur.

Information on the mechanisms involved in tumor resistance has the potential to provide the fundamental basis for novel therapeutic strategies. In this context, an approach that has been extensively investigated is synthetic lethality, which may occur when two gene functions are compromised due to the simultaneous loss/or mutations in both genes, which can lead to cell death (12). Over two decades, this approach has

---

*Correspondence to:* Dr Elza T. Sakamoto-Hojo, Department of Biology, Faculty of Philosophy, Sciences and Letters at Ribeirão Preto, University of São Paulo, 3900 Bandeirantes Avenue, Ribeirão Preto, São Paulo 14040-901, Brazil  
E-mail: etshojo@usp.br

**Key words:** PARP-1 inhibition, glioblastoma, temozolomide, *PTEN*, *MGMT*, predictive biomarker

been studied to explore the potential of applying PARP inhibition to cancer therapy (12-14), and the PARP-BRCA interaction provides the first successful example of clinical application in patients with breast/ovarian cancer (15-17). The increased susceptibility of breast cancer cells to PARP inhibitor (PARPi) is thought to result from the association between PARP-1, BER and homologous recombination (HR) repair pathways (17). Furthermore, the sensitivity to PARPi has also been reported in cells that present other genetic alterations affecting HR, including mutations in the phosphatase and tensin homologue deleted on chromosome ten (*PTEN*) gene (18) and ataxia telangiectasia mutated (*ATM*) deficiency (19). *PTEN* is a tumor-suppressor gene, which appears to play a role in astrocytomas (20). Changes in the *PTEN* gene, including the loss of heterozygosity, mutation and methylation, have been identified in at least 60% of GBMs (21). In addition to the phosphatase activity that is attributed to PTEN (22), it has been demonstrated that this protein is associated with the centromere, specifically interacting with the CENP-C region, becoming a critical controller of the dynamic organization of the centromere and promoting genomic stability. This can also lead to defects in double-strand break (DSB) repair when *PTEN* is absent, suggesting its role in the HR pathway (23). The authors of the aforementioned study also demonstrated that PTEN acts at the chromatin level, influencing the remodeling of the region encompassing the *RAD51* promoter, thereby controlling *RAD51* transcription by E2F-1. However, conflicting and limited results have been indicated regarding *PTEN* influence on the expression of *RAD51* and its paralogs, as well as on HR efficiency (24). In glioma cells, it has previously been demonstrated that a disruption of HR components (*RAD51* and *BRCA2*) sensitizes these cells to alkylating agents, and it has been demonstrated that the inhibitor of PARP-1 (olaparib) increases cell death (25).

The genetic heterogeneity of GBM tumors is well recognized in the literature, but whether PTEN and MGMT status influence GBM response to treatment with TMZ combined with a PARP-1 inhibitor, has not yet been fully determined. The genetic changes present in tumor cells may contribute to drug sensitivity; therefore, it is relevant to investigate molecular signatures that represent potential predictive markers of susceptibility to therapies for patients with GBM.

The present study hypothesized that PARP-1 inhibition may increase the cytotoxicity of TMZ-induced lesions in GBM cells due to the role of the enzyme in damage responses and multiple DNA repair pathways. Therefore, the present study investigated whether these mechanisms can be influenced by MGMT and *PTEN* status. While it is well established that MGMT is the main factor that leads to GBM resistance to TMZ, the impact of *PTEN* deficiency in repair pathways, and the consequences of PARP-1 inhibition and *PTEN* silencing (or deficiency), in terms of synthetic lethality, was also evaluated in TMZ-treated GBM cells.

In the present study, GBM cell lines presenting different *PTEN* status and MGMT activity were used, and the results of combined treatments (TMZ plus PARPi - NU1025) were analyzed. The results demonstrated the effectiveness of these treatments in sensitizing TMZ-resistant and -sensitive cells, independent of MGMT activity. However, PARP-1 inhibition was unable to sensitize U87MG TMZ-sensitive cells, either as

a single treatment, or in the TMZ-combined treatment. The cellular responses to TMZ/NU1025 in TMZ-resistant cells involved antiproliferative activity, G2/M arrest, DSBs and the induction of apoptosis. Regarding the influence of *PTEN* status on drug-treated cells, the results of the current study indicated that *PTEN*-silenced LN18 cells did not exhibit sensitization to PARPi tested alone, indicating an absence of synthetic lethality. Furthermore, the responses to the combined treatment (TMZ plus PARPi) were also independent of *PTEN* status. PARPi combined with TMZ treatment (during three days) caused a strong reduction in cell viability at 20 days, in contrast to cells treated with TMZ alone. Therefore, the combination of PARPi with TMZ was revealed to be a promising strategy that can be used to overcome TMZ-resistance in GBM cells, and these effects are independent of *MGMT* and *PTEN*.

## Materials and methods

**Cell lines and culture.** T98G (CRL-1690; glioblastoma), LN18 (CRL-2610; glioblastoma) and U87MG (HTB-14<sup>TM</sup>; glioblastoma of unknown origin) cell lines were purchased from American Type Culture Collection, and U251MG (glioblastoma) was provided by Guido Lenz Department of Biophysics, Federal University of Rio Grande do Sul (UFRGS - Porto Alegre, RS, Brazil) (26). All cell lines were authenticated (STR profiling method) and evaluated for mycoplasma contamination prior to the experiments. The cell lines differ regarding the proficiency for the *TP53* gene, and the activity of the MGMT repair enzyme (T98G and LN18 are *TP53* deficient with high MGMT activity; U87MG is *TP53* proficient and lacks MGMT activity; U251MG is *TP53* deficient with no MGMT activity). T98G, U251MG and U87MG are *PTEN*-mutated but LN18 is *PTEN* wild-type (27,28). T98G and LN18 cells, which are MGMT proficient, are resistant to TMZ treatment, indicating IC<sub>50</sub> values >500  $\mu$ M, unlike U87MG and U251MG cells, which are sensitive (IC<sub>50</sub> values <50  $\mu$ M) (27). Therefore, T98G and LN18 are referred to as resistant cells, whereas U87MG and U251MG are referred to as sensitive to TMZ in the present study.

Cells were kept frozen in liquid nitrogen. After thawing, the cells were cultured in HAM F10/DMEM (1:1) medium (Sigma-Aldrich; Merck KGaA) supplemented with 10% FBS (Sigma-Aldrich; Merck KGaA), penicillin (100 U/ml; Sigma-Aldrich; Merck KGaA), and streptomycin (100 mg/ml; Sigma-Aldrich; Merck KGaA) at 37°C in a humidified 5% CO<sub>2</sub> incubator.

**Cell treatment with TMZ and PARP-1 inhibitor.** For TMZ treatment (TEMODAL- Shering-Plough Corp.), the concentrations used in the present study were based on previous results (9,27); those selected were above the values of IC<sub>50</sub> calculated for the cell lines, although previous reports show that concentrations of 10-25  $\mu$ M are equivalent to those found in the spinal fluid of patients after treatment (29,30). Therefore, TMZ-resistant cells (T98G and LN18; MGMT-proficient) were treated with 100 and 200  $\mu$ M of TMZ, while TMZ-sensitive cells (U87MG and U251MG; MGMT-deficient) were treated with 10  $\mu$ M.

For PARP-1 inhibition, the NU1025 agent (Sigma-Aldrich; Merck KGaA) was used in the current study, since it has been

successfully used by several authors (31-35). Two concentrations of NU1025 (NU-100 and 200  $\mu$ M) were added 20 min prior to TMZ treatment. MGMT inhibition was achieved using 30  $\mu$ M of O6-BG inhibitor (Sigma-Aldrich; Merck KGaA) 1 h prior to TMZ treatment. All drugs remained in cell cultures until subsequent experimentation. To test the PARP-1 inhibition efficiency by NU1025 agent, the cells were treated with H<sub>2</sub>O<sub>2</sub> (20 mM) for 10 min following NU1025 incubation, and were subsequently evaluated using immunofluorescent detection for poly-ADP-ribose (PAR) polymers.

**Small interfering (si)RNA transfection.** LN18 cells were transfected with *PTEN* siRNA (cat. no. sc-29459; Santa Cruz Biotechnology, Inc.) and a non-specific siRNA control (cat. no. sc-37007; Santa Cruz Biotechnology, Inc.) at a final concentration of 100 nM with Lipofectamine 2000 (Invitrogen; Thermo Fisher Scientific, Inc.), according to the manufacturer's protocol. A control siRNA was used as a negative control, consisting of a scrambled sequence (20-25 nucleotides) that does not target any known genes in the target cells. The efficiency of LN18 siRNA transfected cells was confirmed using western blot analysis. Treatment with NU1025 and TMZ was performed 72 h after transfection, and the experiments were repeated three times.

**Protein isolation and western blot analysis.** Cells were lysed in 200  $\mu$ l of the RIPA buffer reagent (Thermo Fisher Scientific, Inc.) supplemented with Halt™ Protease Inhibitor Cocktail kit (Thermo Fisher Scientific, Inc.). Protein concentration was determined using BCA Protein Assay reagents (Thermo Fisher Scientific, Inc.), according to the manufacturer's protocol. Proteins (30  $\mu$ g) were separated by electrophoresis in NuPAGE 4-12% Bis-Tris gel (Thermo Fisher Scientific, Inc.) and blotted onto a PVDF membrane (Thermo Fisher Scientific, Inc.). Samples were incubated in blocking buffer before the addition of the primary antibody. The immuno-detection was accomplished using a WesternBreeze Chemiluminescent kit (Thermo Fisher Scientific, Inc.). The antibodies used were as follows: anti-mouse PTEN (cat. no. 9556; dilution 1:1,000), anti-rabbit phospho-AKT<sup>(Ser473)</sup> (cat. no. 9271; dilution 1:500), anti-rabbit AKT (cat. no. 9272; dilution 1:1,000), anti-rabbit MGMT (cat. no. 2739; dilution 1:1,000), and anti-rabbit  $\beta$ -actin (cat. no. 4967; dilution 1:2,000) or anti-rabbit  $\beta$ -tubulin (cat. no. 2146; dilution 1:1,000), which were used as endogenous controls for normalization. All antibodies were purchased from Cell Signaling Technology, Inc. The chemiluminescence detection was performed using the ImageQuant LAS 500 (GE Healthcare Life Sciences) and quantified using Gel-Pro Analyzer 4.0 software (Media Cybernetics, Inc.).

**Cell proliferation assay.** GBM cells (T98G, LN18, U87MG and U251MG) were seeded (2,000 cells/well) in 12-well plates and incubated at 37°C. After 24 h, cells were treated with TMZ and NU1025, and cell viability was evaluated after 7 days. Cells were subsequently washed with PBS followed by incubation with XTT reagent kit as recommended by the manufacturer's protocol (Roche Molecular Diagnostics).

**Clonogenic assay.** A clonogenic assay was performed according to Franken *et al* (36). After seeding triplicates of

T98G and LN18 cells in 6-well plates (1,000 cells/well), drug treatments were performed. Approximately 10 days after treatment, cells were washed in PBS, fixed (methanol) and stained with Giemsa (20 min at room temperature). The colonies with >50 cells were counted using a stereomicroscope at 16x magnification (Carl Zeiss).

**Cell cycle analysis.** After TMZ and NU1025 treatment, T98G and LN18 cells were washed with PBS and fixed in 70% ethanol, stained for 15 min (37°C) with a solution containing propidium iodide (PI) (5  $\mu$ g/ml) and RNase (50  $\mu$ g/ml) and analyzed in a Guava EasyCyte Mini System (Merck KGaA), according to the manufacturer's protocol. Percentages of cells undergoing G0/G1, S, or G2/M phase were collected on days one and three after treatment and analyzed using Guava Personal Cell Analysis system (Merck KGaA).

**Apoptosis assays and Annexin-V staining.** Apoptosis detection was evaluated at 3 and 5 days following TMZ and NU1025 treatment. Apoptosis induction was measured using the Guava Nexin reagent (Merck KGaA), according to manufacturer's protocol. The samples were processed using flow cytometry and analyzed using Guava Personal Cell Analysis system (Merck KGaA).

**Flow cytometry for  $\gamma$ H2AX and PAR analysis.** For  $\gamma$ H2AX and PAR (poly-ADP-ribose) immunostaining, cells were fixed with paraformaldehyde (3%) and permeabilized (Triton-X 0.5%). Cells were then incubated with either primary rabbit monoclonal antibody to  $\gamma$ H2AX<sup>(Ser-139)</sup> (cat. no. sc101696; Santa Cruz Biotechnology, Inc.), or anti-mouse pADPr (product code ab14459; Abcam), both diluted (1:400) and incubated for 1 h at 37°C. Cells were then incubated with Alexa Fluor® 488 anti-rabbit IgG (cat. no. A21441; Invitrogen; Thermo Fisher Scientific, Inc.) or Alexa Fluor® 594 anti-mouse IgG (cat. no. A21201; Invitrogen; Thermo Fisher Scientific, Inc.; dilution 1:400) for 30 min at 37°C. The percentage of positive cells was calculated using the Guava Personal Cell Analysis system (Merck KGaA).

**RNA isolation and reverse transcription-quantitative (RT-q) PCR by PCR array.** The transcriptional profiles were analyzed for a set of DNA repair genes and evaluated using RT-qPCR with a customized TaqMan® Assay Mix (Applied Biosystems; Thermo Fisher Scientific, Inc.). Cells were collected at 6 and 24 h post-treatment, and total RNA was isolated using illustra RNAspin Mini (GE Healthcare). RNA integrity was performed using a RNA 6000 Nano kit (Agilent Technologies, Inc.) and Bioanalyzer 2100 (Agilent Technologies, Inc.), following the manufacturer's protocol. The first-strand complementary DNA (cDNA) was synthesized from 1  $\mu$ g of each RNA sample using the SuperScript® VILO™ Master Mix (Invitrogen; Thermo Fisher Scientific, Inc.) according to the manufacturer's protocol. A cDNA pool of three independent experiments was used for the screening of gene expression profiles. The reactions were prepared using TaqMan® Fast Universal PCR Master Mix (Applied Biosystems). The TaqMan® Assay plate used was customized by Thermo Fisher Scientific, Inc., and contained 21 genes (DNA repair pathways) and two reference genes (Table SI). All plates were run on QuantStudio 3

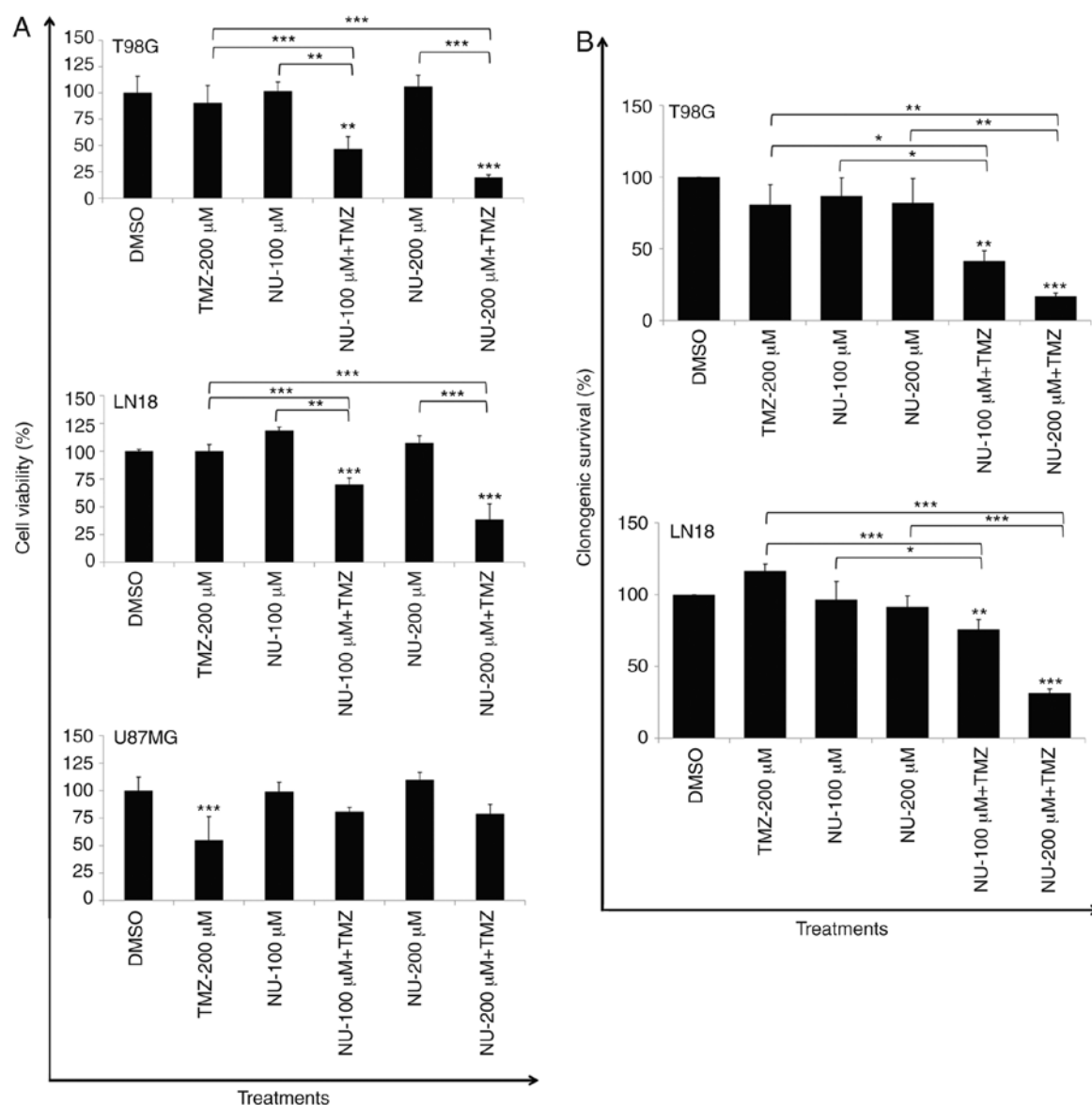


Figure 1. Cytotoxic effects of TMZ and PARPi combined treatments. (A) Cell viability of T98G, LN18 and U87MG cells was evaluated by the XTT assay, after 7 days of NU1025 (NU-100 and NU-200  $\mu$ M) and TMZ (200  $\mu$ M for T98 and LN18; 10  $\mu$ M for U87MG) continuous treatment. (B) Clonogenic survival of T98G and LN18 cells analyzed after 10 days of drug treatments. Values are mean  $\pm$  SD of three independent experiments. Statistical significance compared to control cells (DMSO). \* $P$ <0.05, \*\* $P$ <0.01, \*\*\* $P$ <0.001. Bars correspond to the comparisons between treatments. TMZ, temozolomide; PARPi, poly-ADP-ribose polymerase inhibitor.

Real-Time PCR Systems (Applied Biosystems) and analyzed using QuantStudio™ Design & Analysis Software1.3.1 (Applied Biosystems) using the  $2^{-\Delta\Delta C_q}$  method (37). *TBP* and *HPRT1* genes were used as endogenous controls.

**Statistical analysis.** Statistical analysis was performed using the SigmaStat software (version 3.5; Jandel Scientific Software). A one-way ANOVA, followed by Holm-Sidak multiple comparison tests, was used to establish whether significant differences existed between the groups.  $P$ <0.05 was considered to indicate a statistically significant difference. All experiments were independently performed at least three times and the results are expressed as the mean  $\pm$  standard deviation. Results obtained for gene expression (cDNA pool of three independent experiments) are expressed as fold-change values.

## Results

**PARPi potentiates TMZ-induced cytotoxicity in GBM TMZ-resistant cell lines.** To confirm specific genetic alterations in each cell line, MGMT, PTEN, and AKT protein expression was analyzed (Fig. S1A). Additionally, the p<sup>(ser473)</sup>AKT was evaluated to confirm its activation due to PTEN deficiency in T98G and U87MG cells. To validate PARP-1 inhibition by NU1025, T98G cells were treated with H<sub>2</sub>O<sub>2</sub> (20 mM) prior to NU1025 treatment (100 or 200  $\mu$ M), and PAR levels were assessed using flow cytometry. Following a 10 min incubation, a significant increase in PARP-1 activity (PAR detection) was detected in H<sub>2</sub>O<sub>2</sub>-treated cells, while as expected, NU1025 treatment markedly decreased PAR polymers in response to H<sub>2</sub>O<sub>2</sub> treatment (Fig. S1B). Cells were then treated with TMZ (200  $\mu$ M) and NU1025 (100 or 200  $\mu$ M). As detected using a

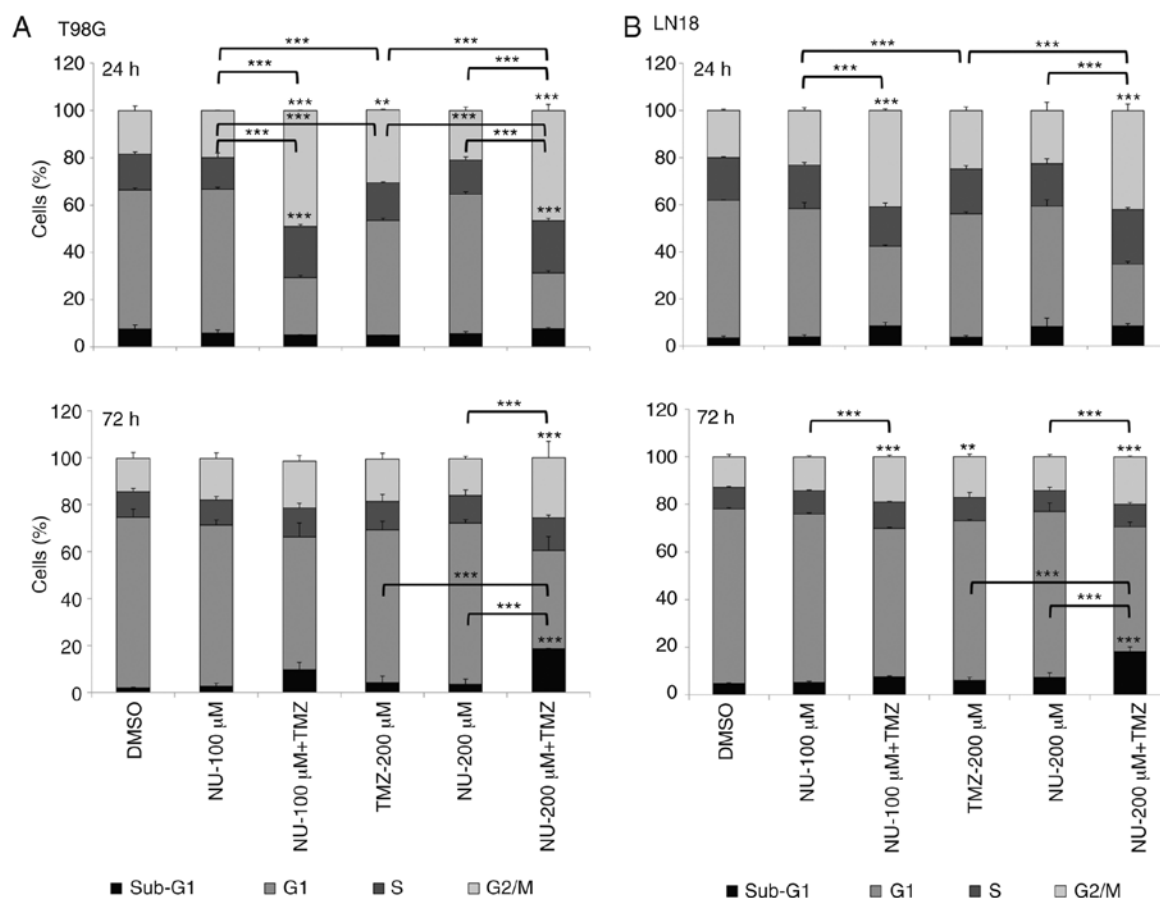


Figure 2. Cell cycle progression of GBM cells after TMZ and PARPi combined treatments. T98G (A) and (B) LN18 cells were treated with NU1025 (NU-100 and NU-200  $\mu$ M) and TMZ (200  $\mu$ M) and cell cycle kinetics was analyzed by flow cytometry after 24 and 72 h of treatments. Values are mean  $\pm$  SD of three independent experiments. Statistical significance compared to control cells (DMSO). \* $P$ <0.01, \*\*\* $P$ <0.001. Bars correspond to the comparisons between treatments. GBM, glioblastoma; TMZ, temozolomide; PARPi, poly-ADP-ribose polymerase inhibitor.

XTT assay, which was performed after 7 days of continuous treatment, the drug combination caused a significant reduction in cell viability in T98G (*PTEN*-mutated) and LN18 cells (*PTEN*-wild type), which are TMZ-resistant (MGMT proficient cells), and this was independent to the *PTEN* status (Fig. 1A). Survival rates were reduced ~4.7- and 3.7-fold following the combined treatment (NU-200  $\mu$ M + TMZ-200  $\mu$ M) for T98G and LN18 cells, respectively, compared with a TMZ single treatment, as evaluated at 10 days after treatment (Fig. 1B). Similar experiments were performed in TMZ-sensitive U87MG cells (*PTEN*-mutated), which did not present MGMT, to analyze their sensitivity to the combined treatment. A marked reduction in cell viability was observed in cells treated with TMZ (10  $\mu$ M, single treatment), and a significant difference was not indicated between TMZ alone and TMZ combined to NU1025 (Fig. 1A).

NU1025 (single treatment) did not demonstrate a cytotoxic effect in *PTEN* proficient (LN18) and deficient cells (T98G and U87MG), indicating that *PTEN* status may not contribute to the synthetic lethality promoted by PARPi in the absence of DNA damage, which is induced by TMZ in GBM cells.

**Combined treatment of PARPi and TMZ induces G2/M blockage and apoptosis.** It has been previously reported that BER intervention by APE1 depletion in T98G cells caused G2/M arrest, DSBs and apoptosis induction in response to TMZ treatment (10). The present study investigated whether the

inhibition of PARP-1 could cause similar effects considering its role in the BER pathway. Whether differences in the *PTEN* status could lead to different drug responses was therefore assessed. T98G and LN18 cells treated with TMZ (200  $\mu$ M) plus NU1025 (100 or 200  $\mu$ M) indicated a significant G2/M block at 24 h after treatment compared with single-treatments (TMZ or NU1025) and control (DMSO) cells. G2/M arrest was maintained after 72 h, compared with NU1025-treated and control cells, either in T98G (NU-200  $\mu$ M + TMZ) and LN18 cells (NU-100 or 200  $\mu$ M + TMZ). Furthermore, only T98G cells treated with NU1025 + TMZ also demonstrated a significant increase in the proportion of S-phase cells observed at 24 h, compared with single-treatments and the control. T98G and LN18 cell lines also revealed a significant increase in the sub-G1 content (DNA fragmentation) following treatment with TMZ plus NU1025 (200  $\mu$ M) in cells collected after 72 h, compared with single drug-treatments or the control group (Fig. 2A and B). The cell cycle blockade may have occurred as a result of DSBs generated by the combined treatment, as evaluated by the detection of  $\gamma$ H2AX-positive cells (6, 24 and 72 h), which were demonstrated to be increased. In these experiments,  $\gamma$ H2AX-positive cells were calculated (average of relative values), as the experimental vs. the control (DMSO), in order to compare the responses between cell lines, taking into account their genetic background, including the *PTEN* status. The results indicated that DSB induction was

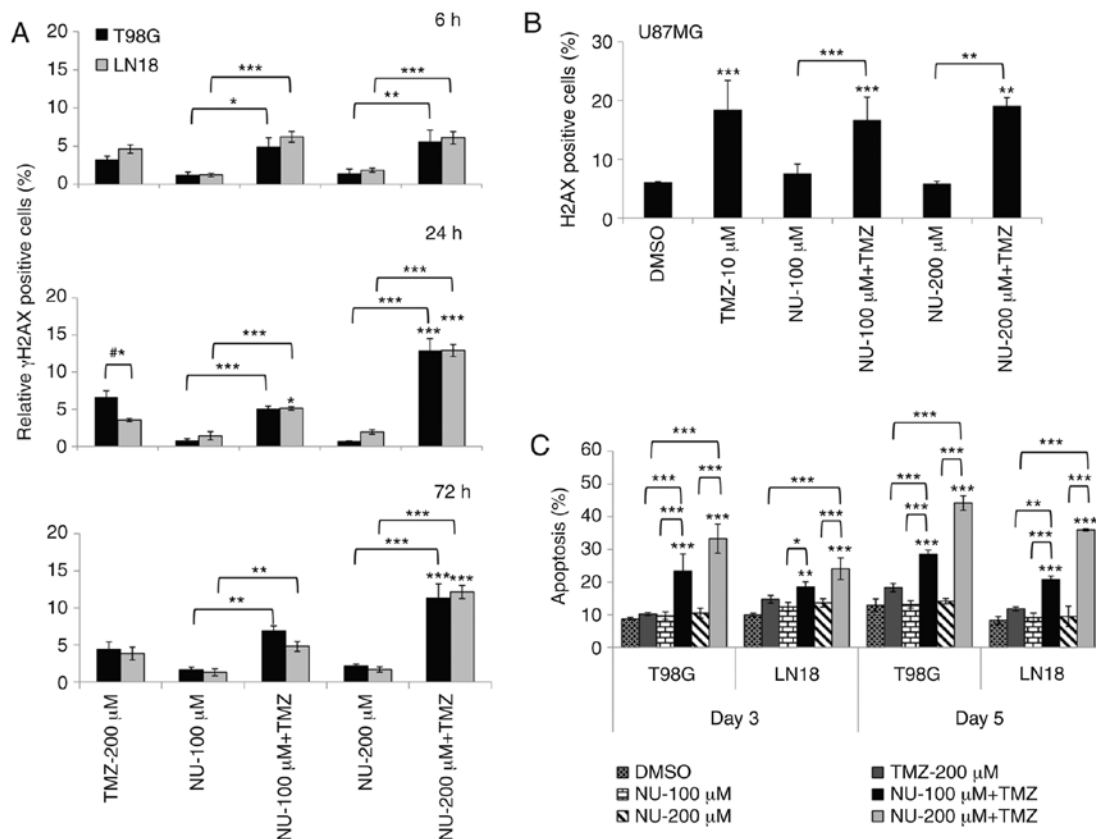


Figure 3. Combined treatments (TMZ and PARPi) induce DSBs and apoptotic cell death. (A) Percentages of  $\gamma$ H2AX-positive staining in T98G and LN18 cells after 6, 24 and 72 h of TMZ (200  $\mu$ M) and NU1025 (NU-100 and NU-200  $\mu$ M) treatment, as analyzed by flow cytometry. (B) Percentages of U87MG  $\gamma$ H2AX-positive cells after 3 days of TMZ (10  $\mu$ M) and NU1025 (NU-100 and NU-200  $\mu$ M) treatment, analyzed by flow cytometry. (C) Apoptosis induction in T98G and LN18 cells after 3 and 5 days of TMZ (200  $\mu$ M) and NU1025 (NU-100 and NU-200  $\mu$ M) treatment analyzed by flow cytometry using Annexin-V reagent. Values are mean  $\pm$  SD of three independent experiments. Statistical significance compared to control cells (DMSO). \* $P$ <0.05, \*\* $P$ <0.01, \*\*\* $P$ <0.001. Bars correspond to the comparisons among treatments. (#\*) correspond to the comparison between cell lines. DSBs, double-strand breaks; TMZ, temozolomide; PARPi, poly-ADP-ribose polymerase inhibitor.

similar in both cell lines (T98G and LN18), except for TMZ single treatment in T98G cells, which presented a greater percentage of  $\gamma$ H2AX-positive cells detected at 24 h (Fig. 3A). These data indicated that differences in the *PTEN* status did not significantly affect the induction of DSBs. The amount of  $\gamma$ H2AX-positive cells increased from 6 to 72 h following the combined treatments, and the reduction in cell viability may be a consequence of a decreased DNA repair that is promoted by PARP inhibition. In U87MG cells, the  $\gamma$ H2AX induction (Fig. 3B) was likely due to the TMZ single-treatment, confirming the lack of response to the combined treatment, as demonstrated by the results of the cell viability assay.

Furthermore, the results of the present study indicated that the responses to DNA damage observed for the combined treatment was different when comparing the two cell lines, since T98G indicated higher levels of apoptosis induction than LN18 cells. This may be due to LN18 being more efficient in DSB repair than T98G cells (Fig. 3C). NU1025 single treatment did not induce changes in the cell cycle kinetics, and did not cause any effect on the induction of DSBs and apoptosis, corroborating the results of cell viability and clonogenic survival.

*PTEN silencing did not affect the efficacy of PARPi plus TMZ-treatment.* Considering the possible involvement of

PTEN in the HR pathway (18), experiments were performed in LN18 *PTEN*-silenced cells to demonstrate the lack of synthetic lethality, since this phenomenon was not observed in *PTEN*-deficient cells (T98G, U251, and U87MG). siRNA *PTEN* LN18 cells indicated a substantial decrease in gene expression (94.7% of knockdown; data not shown), as well as in *PTEN* protein level (Fig. 4A and B). The total-AKT expression was not significantly affected by the *PTEN* silencing, but an increase in p-AKT expression was observed (Fig. 4C and D). This indicates that *PTEN* downregulation promotes the modulation of the PI3K/AKT signaling pathway, and this is supported by the increase in the p-AKT/total-AKT ratio in *PTEN*-silenced cells (Fig. 4D). However, in these cells, *PTEN* downregulation did not significantly influence the responses to PARPi tested as a single agent, and in a combination with TMZ, compared with siSCR cells (transfection control), as evaluated using cell viability (Fig. 4E) and Annexin assays (Fig. 4F). These results indicated that *PTEN* does not contribute to the occurrence of synthetic lethality in GBM cells, and is not crucial for the cytotoxicity induced by the combined treatment (TMZ + NU1025) in LN18 TMZ-resistant cells.

*MGMT repair does not influence the efficiency of PARPi plus TMZ treatment.* To evaluate whether the effects of TMZ

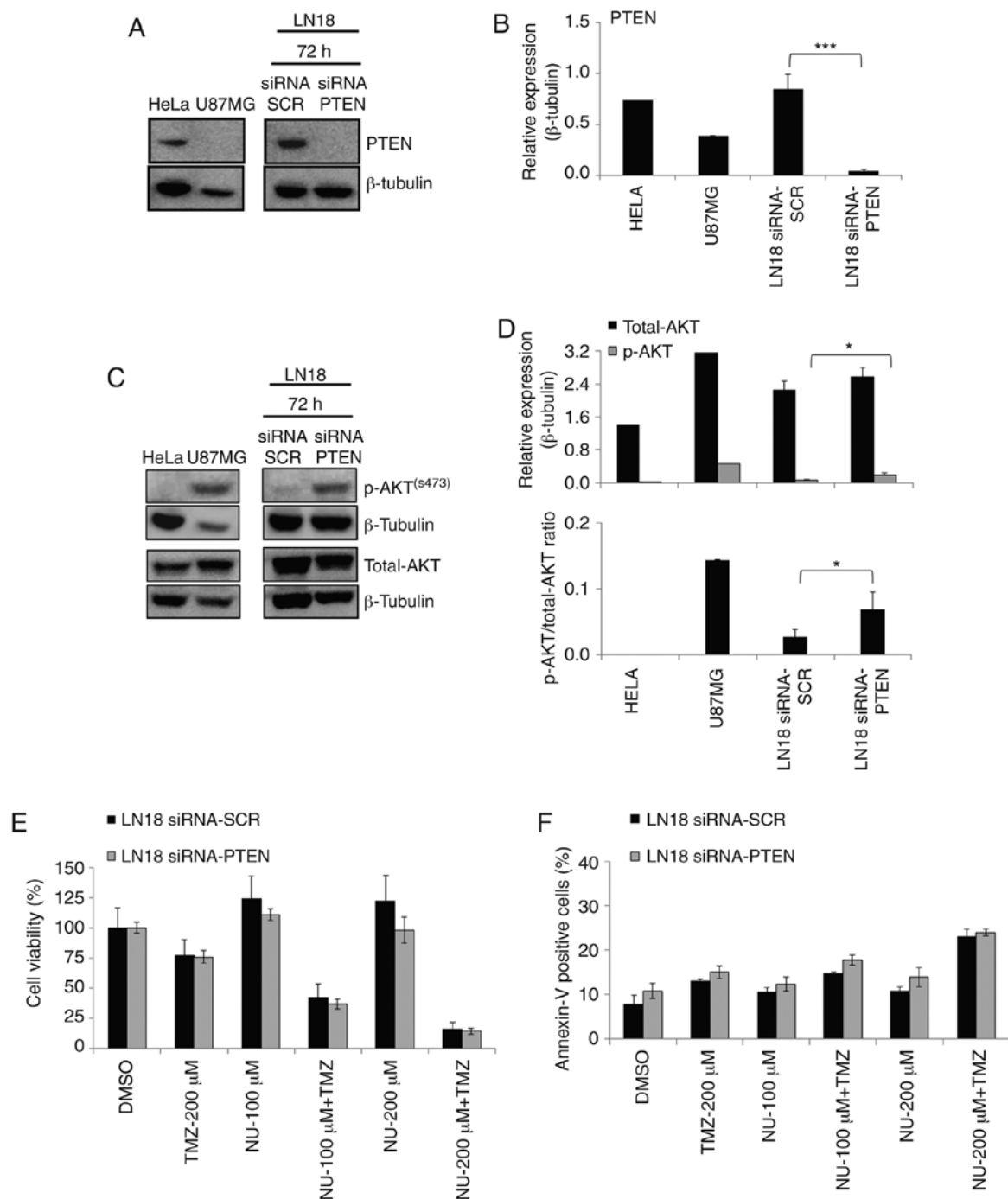


Figure 4. Cellular responses of LN18 *PTEN*-silenced cells to combined treatments. (A) *PTEN* expression and (B) quantification by western blot analysis after 72 h of transfection with SCR (control) or *PTEN* siRNA. (C) p-AKT and total-AKT expression and (D) quantification, as well as p-AKT/total AKT ratio, following 72 h of transfection. U87MG and HeLa cells were used as negative and positive controls for *PTEN* expression, respectively.  $\beta$ -tubulin was used as a loading control. (E) Cell viability of LN18 SCR or *PTEN* siRNA cells treated with TMZ (200  $\mu$ M) and NU1025 (U-100 and U-200  $\mu$ M) analyzed at 7 days after continuous drug treatment, as measured by the XTT assay. (F) Flow cytometric analysis of Annexin-V positive staining in LN18 *PTEN* and SCR silenced cells, analyzed at 3 days after TMZ (200  $\mu$ M) and NU1025 (U-100 and U-200  $\mu$ M) treatment. Values are mean  $\pm$  SD calculated from three independent experiments. Statistical significance: \* $P < 0.05$ , \*\*\* $P < 0.001$ . Bars correspond to comparisons between treatments. *PTEN*, phosphatase and tensin homologue deleted on chromosome ten.

plus NU1025 combined treatment are dependent on MGMT activity, the O6-BG agent was used to inhibit the activity of the enzyme in T98G and LN18 cells. A significant reduction in cell viability was observed in the TMZ/O6-BG and TMZ/O6-BG/NU (100 and 200  $\mu$ M) treated cells. The results indicated that the inhibition of MGMT activity (O6-BG) did not significantly counteract the effectiveness of PARP inhibi-

tion in TMZ-treated cells, since it also contributed to a possible additive effect on cell sensitization (Fig. 5A). Additionally, to test whether MGMT repair influenced the response to PARPi plus TMZ treatment, experiments were performed in U251MG cells, which are deficient for MGMT activity (27), and also carry *TP53* and *PTEN* mutations (28). The results obtained for U251MG cells revealed that MGMT activity does not

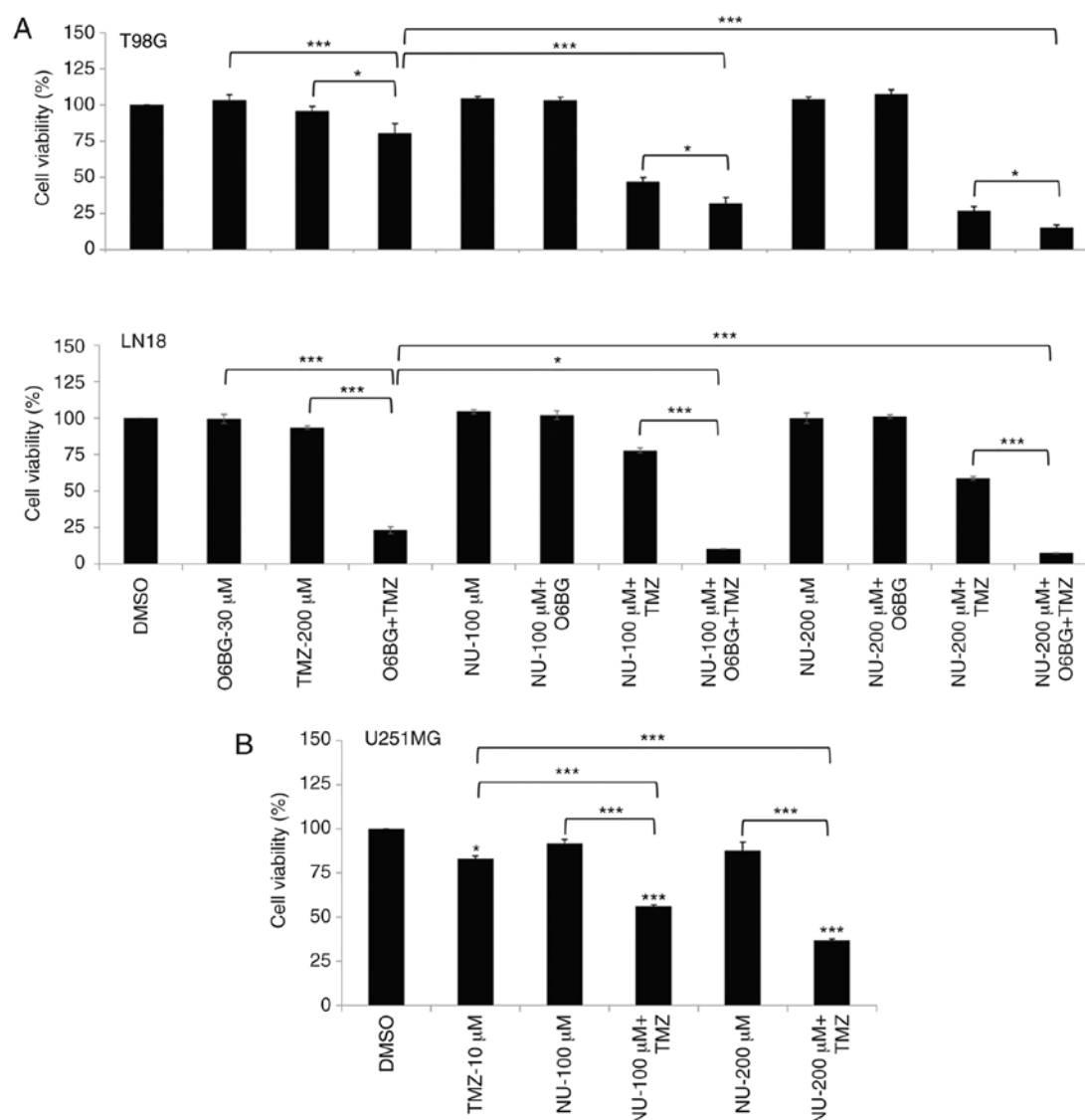


Figure 5. NU1025 enhances the cytotoxic effects of TMZ treatment independently of MGMT activity and does not cause acquired resistance. (A) Cell viability of T98G and LN18 cells after MGMT inhibition (O6-BG agent, 30  $\mu$ M) and continuous treatment with TMZ (200  $\mu$ M) and NU1025 agents (NU-100 and NU-200  $\mu$ M). (B) U251MG viable cells treated with TMZ (10  $\mu$ M) and NU1025 (NU-100 and NU-200  $\mu$ M). The cell viability was evaluated by the XTT assay, after 7 days following treatments. Statistical significance compared to control cells (DMSO). \* $P$ <0.05, \*\*\* $P$ <0.001. Bars correspond to comparisons between treatments. TMZ, temozolomide; MGMT, O<sup>6</sup>-methylguanine DNA methyltransferase.

affect cellular responses to drug treatments, and corroborated the results obtained in T98G and LN18 cells under MGMT inhibition (Fig. 5B). However, the absence of a response observed for U87MG cells suggested the influence of other genetic alteration, since these cells also lack MGMT activity.

**PARPi treatment overcomes TMZ-induced resistance.** Cell viability was also determined following 20 days of recovery time after three consecutive days of TMZ (100 and 200  $\mu$ M) treatment, administered alone or in combination with NU1025 (200  $\mu$ M), to evaluate the occurrence of resistance to the combined treatment. TMZ treatment was unable to reduce cell viability following 20 days. However, a period of three consecutive days of combined treatment (TMZ plus NU-200  $\mu$ M) was efficient to significantly decrease the viability in T98G and LN18 cell lines (Fig. 6), demonstrating the absence of resistance under the conditions tested, and indicating that the induced-lethality was independent to the *PTEN* status. Taken

together, these results demonstrated the effectiveness of the drug combination to sensitize TMZ-resistant tumor cells.

**Transcript expression of GBM cells exposed to TMZ plus PARPi treatment.** To determine the influence of the PARP-1 inhibitor on the recruitment of repair mechanisms in response to TMZ treatment, a gene set of DNA repair genes was selected to evaluate transcriptional expression profiles (6 and 24 h) in LN18 and T98G cell lines. BER (*APEX1*, *PARP1*, *FEN1*, *LIG1*, and *XRCC1*), HR (*BRCA1*, *RAD51*, *RAD51B/C/D* and *LIG4*), non-homologous end joining (NHEJ; *PRKDC* and *XRCC5/6*), nucleotide excision repair (NER; *XPA*, *XPC*, and *XRCC4*), mismatch repair (MMR; *MSH2/3*) and *MGMT* genes were evaluated in the current study. In addition, transcriptional expression of HR genes was compared between the two cell lines, which possess a different *PTEN* status. To establish differential transcript expression, fold-change (Log2) values >1.31 were considered to be the cut off.



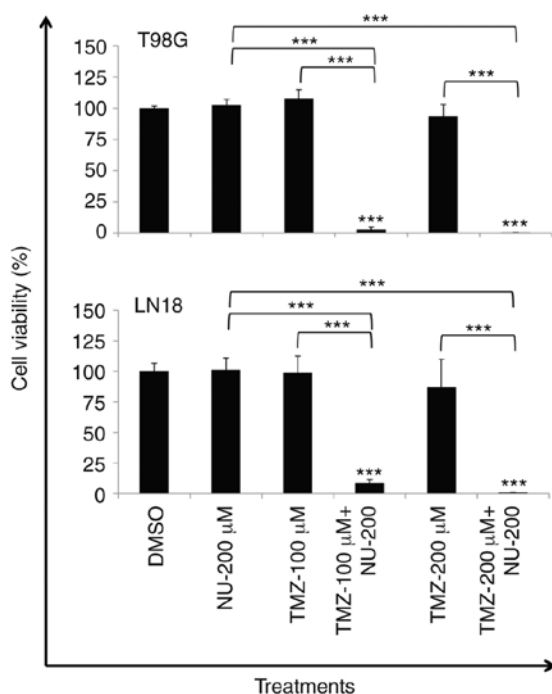


Figure 6. Combined treatment of NU1025 and TMZ does not cause acquired resistance. T98G and LN18 viable cells in response to 3 days of combined or single treatments of TMZ (100 and 200  $\mu$ M) and NU1025 (NU-200  $\mu$ M), following 20 days recovery, evaluated by the XTT assay. Values are mean  $\pm$  SD calculated from results of three independent experiments. \*\*\* $P$  < 0.001. Bars correspond to comparisons between treatments. TMZ, temozolomide.

In the clustering analysis, the two cell lines presented a distinct damage response, however, each cell line was clustered according to the time-point (6 or 24 h), except for T98G NU1025-treated cells evaluated after 24 h (Fig. 7). Regarding DNA repair pathways in T98G *PTEN*-deficient cells, BER (*PARP1*, *FEN1*, and *LIG1*) and HR (*BRCA1* and *RAD51B/C*) genes were indicated to be slightly induced by TMZ (24 h), while the effect of PARP-1 inhibition by NU1025 abolished these responses in the combined treatment (Fig. 7; Table SII). However, LN18 *PTEN*-proficient cells did not exhibit changes in expression in response to treatments (Fig. 7; Table SIII). An upregulation of *RAD51* paralogs (*B* and *C*) was indicated following a single treatment of TMZ in T98G *PTEN*-deficient cells, but the same result was not revealed in LN18 *PTEN*-proficient cells, indicating that there is no correlation between *PTEN* status and the expression of these genes, which are associated with the HR pathway.

## Discussion

Despite a number of studies concerning the use of poly-ADP-ribose polymerase inhibitors (PARPi) as a strategy for cancer treatment (38-40), information on the mechanisms and genetic factors influencing the responses to PARPi and temozolomide (TMZ) combination are still largely undetermined, especially in glioblastoma (GBM). To study this approach and the mechanisms associated with drug responses, four cell lines that present different genetic alterations regarding MGMT activity and *PTEN* genes were analyzed in the current study.

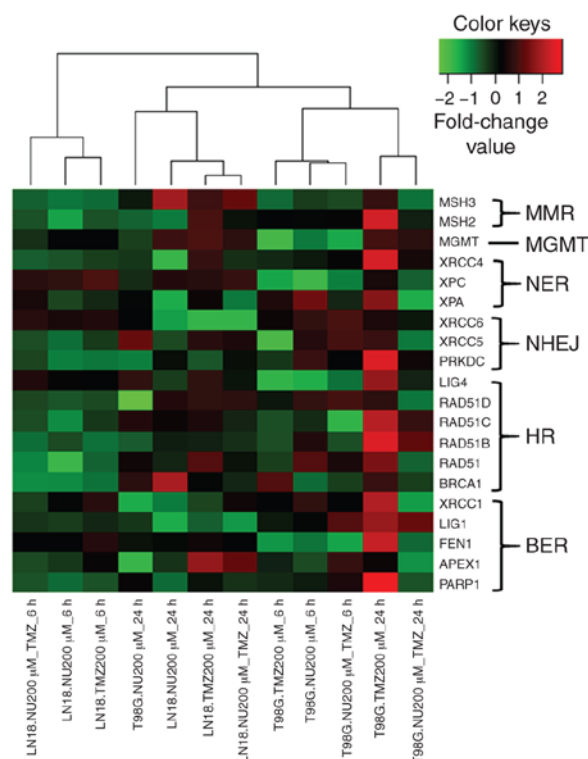


Figure 7. GBM cell lines showing gene expression profiles in response to PARPi and TMZ combination. Hierarchical clustering illustrating a graphical representation of transcript expression profiles for a gene set encompassing the major repair pathways (BER, NER, MGMT, MMR, HR and NHEJ), as analyzed in LN18 and T98G cells treated with TMZ (200  $\mu$ M) and NU1025 (200  $\mu$ M) for 6 and 24 h. The genes and samples were grouped by using Pearson's correlation, according to the similarity of expression level. Upregulated and downregulated genes are represented in red and green colors, respectively; black represents a lack of differential expression. Variations in the color intensity represent different levels of transcript expression. GBM, glioblastoma; TMZ, temozolomide; BER, base excision repair; NER, nucleotide excision repair; MGMT, O<sup>6</sup>-methylguanine DNA methyltransferase; MMR, mismatch repair; HR, homologous recombination; NHEJ, non-homologous end joining.

The results indicated that the combined treatment (TMZ plus NU1025) was effective in reducing the cell viability and clonogenic survival rates presented by TMZ-resistant cells (T98G and LN18, which are MGMT-proficient). The potentiating effects of the TMZ + PARPi combination treatment occurred independently to MGMT activity, as observed in U251MG TMZ-sensitive (MGMT-deficient) and MGMT-inhibited cells (T98G and LN18 cell lines). The drug combination caused a G2/M arrest due to the generation of double-strand breaks (DSBs) (possibly via the conversion of N-methylpurine lesions, which were not removed due to repair intervention by PARPi), leading to the induction of apoptosis in T98G and LN18 cells. In these cells, increased amount of unrepaired DNA damage was caused by the inhibition of PARP-1 by NU1025, leading to cell death following drug treatments.

However, these responses were not observed in TMZ-sensitive U87MG cells, in which MGMT enzyme activity is absent, in contrast to the results reported by Tentori *et al* (41), using another PARPi (GPI 15427). In the present study, the decrease observed in cell viability in U87MG cells occurred as a consequence of TMZ-induced DSBs in the combined treatments. Erice *et al* (42), demon-

strated that MGMT-proficient melanoma cells, strongly responded to the combination of TMZ and PARPi. For GBM, a number of studies have reported conflicting results regarding markers of response to PARP inhibitors combined with TMZ, including MGMT, PARP-1 or PTEN expression (41-44), emphasizing the importance of these studies regarding the influence of genetic alterations in drug responses. LN18 (PTEN-proficient) and T98G (PTEN-mutant) cells present high MGMT activity, demonstrating high resistance to TMZ, even at concentrations of 100-200  $\mu$ M, and they were sensitized only by the combined treatment. On the other hand, U87MG and U251MG cells (MGMT-deficient; *PTEN*-mutant) were more sensitive to TMZ (10  $\mu$ M), and none of them were affected by PARPi tested alone. However, only U251MG cells were sensitized upon the combined treatment. Thus, regardless of TMZ concentration, PTEN-deficient cells presented different responses to the TMZ and PARPi combined treatment. The current results in U87MG cells suggest a possible influence of additional genetic alterations, since MGMT activity and the *PTEN* status did not interfere in the efficiency of the combined treatment (PARPi + TMZ). Alterations in *TP53* may also cause impact on drug responses and may distinguish these cells (U87MG is wild-type while T98G, LN18 and U251MG are mutant for this gene). It has been demonstrated that radiation-induced changes in transcript profiles of GBM cell lines are dependent on the functional status of *TP53* (45). It has also been reported that *TP53* influences the differential sensitivity of GBM cell lines to combined treatments, including topoisomerase I inhibitor topotecan, radiation therapy, and PARPi (such as NU1025) (35). Zaky *et al* (46) revealed that *TP53* regulated *APE1* transcriptional expression in colorectal adenocarcinoma tumor cells, which was also supported by a study performed by Poletto and colleagues (47) in normal and transformed human fibroblasts. In a previous study, the impact of *APE1* gene silencing was assessed in terms of the TMZ response, and while U87MG cells did not exhibit sensitization to TMZ treatment, T98G was significantly sensitized by *APE1* downregulation (10). It has been indicated that *APE1*/CHK2 signaling is associated with the coordination of DSB repair, facilitating homologous recombination (HR); however, where there is low *APE1* expression, non-homologous end joining (NHEJ) becomes the prevalent repair pathway (48). The authors showed that U87MG cells presented a low basal *APE1* protein expression, and on the basis of this information (48), it can be suggested that the error-prone NHEJ might be a predominant repair pathway in these cells, explaining the lack of responses to PARP-1 inhibition in the present study. Therefore, when studying different cell lines, determining the genetic background of each GBM cell line is critical to understand the responses to PARP-1 inhibition.

In the present study, the influence of *PTEN* status was studied in T98G (*PTEN*-mutated) and LN18 (*PTEN*-wild type) cell lines, and these cells presented similar responses regarding G2/M blockade and DSB induction caused by the combined treatments, regardless of the *PTEN* status and AKT activation. T98G cells (PTEN-deficient) demonstrated a reduction in cell viability and induction of apoptosis that were slightly more pronounced than LN18 cells

(PTEN-proficient) in response to the combined treatment, suggesting some survival pathway or differential damage tolerance between the cell lines, which may have been due to different inherent genetic alterations in these tumor cells. PTEN has been a subject of controversial studies regarding its role in HR efficiency (24). Thus, *PTEN* knockdown experiments by siRNA were conducted to confirm whether the lack of this gene function could contribute to the occurrence of synthetic lethality, or interfere in the combined treatment, considering the possible involvement of PTEN in the HR pathway (18). *PTEN* gene silencing in LN18 did not modify the cellular responses in terms of viability and apoptosis induction, suggesting that this gene did not cause any impact in the responses of the two cell lines to the NU1025 single- or combined treatment (TMZ + NU1025), although the relevance of PTEN roles had been recognized regarding its participation in the PI3K-AKT signaling pathway, and regulation of the G2/M checkpoint, which is associated with genomic instability in tumor cells (49,50). Conflicting conclusions have been reported regarding the role of *PTEN* in drug responses. This may be due to the fact that cancer cells, which have been developed within the context of a genotype with a *PTEN* mutation, accumulate secondary genetic aberrations, differing from cells in which *PTEN* has been experimentally removed (24,51). This may explain the responses to drug treatments that are observed in *PTEN*-silenced LN18 cells.

The transcript expression profiles of a gene set, whose genes represent the major repair pathways (BER, NER, MGMT, MMR, HR and NHEJ), were also examined, since multiple DNA repair pathways can affect the cellular sensitivity to damage caused by methylating agents (52,53). The results revealed that following a 24-h treatment (after one cell doubling), T98G cells treated with TMZ exhibited a number of upregulated genes, including *PARP1*, *FEN1* and *LIG1* (BER), *BRCA1*, *RAD51B/C* (HR), *PRKDC* (NHEJ) and *XRCC4* (NER), while most genes were downregulated or unmodulated at 6 h after treatment. LN18 cells did not exhibit changes in expression profiles for the whole gene set. In other studies, the expression of HR genes (*BRCA1*, *BRCA2*, *RAD51* and *FANCD2*) were also markedly increased in U251MG and A172 cells at 48 h after TMZ treatment, but only *BRCA1* was induced in U87MG cells, suggesting a more effective DNA repair capacity in U251MG and A172 than U87MG cells (54). The expression of *RAD51* and its paralogs did not change in LN18 *PTEN*-proficient cells, which was different to the effect in T98G *PTEN*-deficient cells, which presented an upregulation of *RAD51B/C*. In a previous study, U251MG cells (*PTEN*-mutated) exposed to ionizing radiation (IR) indicated *RAD51 foci*, suggesting a functional HR (48). This finding indicated a negligible PTEN influence on *RAD51* transcript expression in GBM cells. These results also revealed that cell responses to TMZ treatment may differ among cell lines depending on their genetic background. Furthermore, for transcript gene expression, the hierarchical cluster indicated that the cell lines with differences in *PTEN* status (T98G and LN18) were grouped separately, according to time-point (6 or 24 h). These observations reinforce the relevance of the genetic background inherent to each cell line and indicated that cell

responses to drug treatment cannot be driven by a single genetic alteration, including *PTEN* status.

Regarding the PARPi effect on gene expression profiles, NU1025 was effective in inducing a downregulation of the majority of genes in TMZ-treated T98G cells. Since PARP-1 and PARylation serve an important role in the orchestration of the early steps of DNA damage responses, damage signaling and cross-talk with DNA repair pathways (52,55,56), the alterations in transcript expression may be associated with the slight sensitization achieved in T98G cells in response to the combined treatment (TMZ + NU1025), compared with LN18 cells.

In the present study, the survival rates following 20 days (recovery time following cell treatment with TMZ plus PARPi along 3 consecutive days) were close to zero in both cell lines, strongly indicating the efficiency of PARP-1 inhibition in cell death, regardless of *PTEN* status. PARPi in TMZ-treated cells may act to avoid the activation of DNA repair mechanisms, which, as suggested by Ströbel *et al* (48) and Nagel *et al* (57), can lead to an adaptive response to TMZ.

In conclusion, the present study highlights the therapeutic potential of PARPi and TMZ combination for GBM treatment, demonstrating that TMZ-resistant GBM cells, due to the high MGMT activity (known as the main predictor of TMZ response in GBM), can be sensitized by the combination of PARPi with TMZ treatment. The results revealed that *PTEN* gene status and MGMT activity are not genetic predictive markers for the responses to TMZ/PARPi combination in GBM, even though the results with U87MG TMZ-sensitive cells, which were not sensitized to the combined treatment, suggest that other genetic alterations (inherent to the genetic background) may influence the success of the combined treatment. Additionally, *PTEN* did not influence the expression of HR genes, and its down-regulation or deficiency did not sensitize GBM cells to the PARPi single-treatment used in the present study, indicating an absence of synthetic lethality.

### Acknowledgements

The authors are indebted to Mr Luiz A. Costa Jr. for the technical assistance, and Natalia C.S. Moreira for helping with the identification of the cell lines. Our special gratitude to Professor Dr Aguinaldo L. Simões and Mrs Maria do Carmo T. Canas for performing authentication of the GBM cell lines.

### Funding

We acknowledge the financial support from São Paulo Research Foundation (FAPESP, Brazil, grant nos: 2013/12033-0, 2016/17862-3 and 2013/09352-7), National Council for Scientific and Technological Development (CNPq, Brazil) and Coordination for the Improvement of Higher Education Personnel (CAPES, Brazil).

### Availability of data and materials

The datasets used during the present study are available from the corresponding author upon reasonable request.

### Authors' contributions

APM carried out the experimental design, performance of the experiments and analyses of all samples, interpreted the data and wrote the manuscript; SCGL assisted in various experiments. PRDVG participated in the experimental design, data interpretation and revised the manuscript. DJX conducted the qPCR array experiments and data analysis. ETSJ supervised the research work and experimental design, participated in the data collection and interpretation and manuscript preparation. All authors read and approved the manuscript and agree to be accountable for all aspects of the research in ensuring that the accuracy or integrity of any part of the work are appropriately investigated and resolved.

### Ethics approval and consent to participate

Not applicable.

### Patient consent for publication

Not applicable.

### Authors' information

Elza Tiemi Sakamoto-Hojo, ORCID: 0000-0002-1383-3314.

### Competing interests

The authors declare that they have no competing interests.

### References

- Ostrom QT, Gittleman H, Fulop J, Liu M, Blanda R, Kromer C, Wolinsky Y, Kruchko C and Barnholtz-Sloan JS: CBTRUS statistical report: Primary brain and central nervous system tumors diagnosed in the united states in 2008-2012. *Neuro Oncol* 17 (Suppl 4): iv1-iv62, 2015.
- Thakkar JP, Dolecek TA, Horbinski C, Ostrom QT, Lightner DD, Barnholtz-Sloan JS and Villano JL: Epidemiologic and molecular prognostic review of glioblastoma. *Cancer Epidemiol Biomarkers Prev* 23: 1985-1996, 2014.
- Wick W, Osswald M, Wick A and Winkler F: Treatment of glioblastoma in adults. *Ther Adv Neurol Disord* 11: 1756286418790452, 2018.
- Dresemann G: Temozolomide in malignant glioma. *OncoTargets Ther* 3: 139-146, 2010.
- Mutter N and Stupp R: Temozolomide: A milestone in neuro-oncology and beyond? *Expert Rev Anticancer Ther* 6: 1187-1204, 2006.
- Cabrini G, Fabbri E, Lo Nigro C, Dececchi MC and Gambari R: Regulation of expression of O<sup>6</sup>-methylguanine-DNA methyltransferase and the treatment of glioblastoma (Review). *Int J Oncol* 47: 417-428, 2015.
- Yoshimoto K, Mizoguchi M, Hata N, Murata H, Hatae R, Amano T, Nakamizo A and Sasaki T: Complex DNA repair pathways as possible therapeutic targets to overcome temozolomide resistance in glioblastoma. *Front Oncol* 2: 186, 2012.
- Wallace SS, Murphy DL and Sweasy JB: Base excision repair and cancer. *Cancer Lett* 327: 73-89, 2012.
- Montaldi AP and Sakamoto-Hojo ET: Methoxyamine sensitizes the resistant glioblastoma T98G cell line to the alkylating agent temozolomide. *Clin Exp Med* 13: 279-288, 2013.
- Montaldi AP, Godoy PR and Sakamoto-Hojo ET: APE1/REF-1 down-regulation enhances the cytotoxic effects of temozolomide in a resistant glioblastoma cell line. *Mutat Res Genet Toxicol Environ Mutagen* 793: 19-29, 2015.
- Liu L and Gerson SL: Therapeutic impact of methoxyamine: Blocking repair of abasic sites in the base excision repair pathway. *Curr Opin Investig Drugs* 5: 623-627, 2004.

12. Lord CJ, Tutt AN and Ashworth A: Synthetic lethality and cancer therapy: Lessons learned from the development of PARP inhibitors. *Annu Rev Med* 66: 455-470, 2015.
13. Hartwell LH, Szankasi P, Roberts CJ, Murray AW and Friend SH: Integrating genetic approaches into the discovery of anticancer drugs. *Science* 278: 1064-1068, 1997.
14. Bhattacharjee S and Nandi S: DNA damage response and cancer therapeutics through the lens of the fanconi anemia DNA repair pathway. *Cell Commun Signal* 15: 41, 2017.
15. Bryant HE, Schultz N, Thomas HD, Parker KM, Flower D, Lopez E, Kyle S, Meuth M, Curtin NJ and Helleday T: Specific killing of BRCA2-deficient tumours with inhibitors of poly(ADP-ribose) polymerase. *Nature* 434: 913-917, 2005.
16. Farmer H, McCabe N, Lord CJ, Tutt AN, Johnson DA, Richardson TB, Santarosa M, Dillon KJ, Hickson I, Knights C, *et al*: Targeting the DNA repair defect in BRCA mutant cells as a therapeutic strategy. *Nature* 434: 917-921, 2005.
17. Helleday T: The underlying mechanism for the PARP and BRCA synthetic lethality: Clearing up the misunderstandings. *Mol Oncol* 5: 387-393, 2011.
18. Mendes-Pereira AM, Martin SA, Brough R, McCarthy A, Taylor JR, Kim JS, Waldman T, Lord CJ and Ashworth A: Synthetic lethal targeting of PTEN mutant cells with PARP inhibitors. *EMBO Mol Med* 1: 315-322, 2009.
19. Weston VJ, Oldreive CE, Skowronska A, Oscier DG, Pratt G, Dyer MJ, Smith G, Powell JE, Rudzki Z, Kearns P, *et al*: The PARP inhibitor olaparib induces significant killing of ATM-deficient lymphoid tumor cells in vitro and in vivo. *Blood* 116: 4578-4587, 2010.
20. Ohgaki H and Kleihues P: Genetic pathways to primary and secondary glioblastoma. *Am J Pathol* 170: 1445-1453, 2007.
21. Verhaak RG, Hoadley KA, Purdom E, Wang V, Qi Y, Wilkerson MD, Miller CR, Ding L, Golub T, Mesirov JP, *et al*: Cancer genome atlas research network: Integrated genomic analysis identifies clinically relevant subtypes of glioblastoma characterized by abnormalities in PDGFRA, IDH1, EGFR, and NF1. *Cancer Cell* 17: 98-110, 2010.
22. Salmena L, Carracedo A and Pandolfi PP: Tenets of PTEN tumor suppression. *Cell* 133: 403-414, 2008.
23. Shen WH, Balajee AS, Wang J, Wu H, Eng C, Pandolfi PP and Yin Y: Essential role for nuclear PTEN in maintaining chromosomal integrity. *Cell* 128: 157-170, 2007.
24. Lester A, Rapkins R, Nixdorf S, Khasraw M and McDonald K: Combining PARP inhibitors with radiation therapy for the treatment of glioblastoma: Is PTEN predictive of response? *Clin Transl Oncol* 19: 273-278, 2016.
25. Quiros S, Roos WP and Kaina B: Rad51 and BRCA2-New molecular targets for sensitizing glioma cells to alkylating anticancer drugs. *PLoS One* 6: e27183, 2011.
26. Filippi-Chiela EC, Thomé MP, Bueno e Silva MM, Pelegrini AL, Ledur PF, Garicochea B, Zamin LL and Lenz G: Resveratrol abrogates the temozolomide-induced G2 arrest leading to mitotic catastrophe and reinforces the temozolomide-induced senescence in glioma cells. *BMC Cancer* 13: 147, 2013.
27. Hermisson M, Klumpp A, Wick W, Wischhusen J, Nagel G, Roos W, Kaina B and Weller M: O6-methylguanine DNA methyltransferase and p53 status predict temozolomide sensitivity in human malignant glioma cells. *J Neurochem* 96: 766-776, 2006.
28. Ishii N, Maier D, Merlo A, Tada M, Sawamura Y, Diserens AC and Van Meir EG: Frequent co-alterations of TP53, p16/CDKN2A, p14ARF, PTEN tumor suppressor genes in human glioma cell lines. *Brain Pathol* 9: 469-479, 1999.
29. Ostermann S, Csajka C, Buclin T, Leyvraz S, Lejeune F, Decosterd LA and Stupp R: Plasma and cerebrospinal fluid population pharmacokinetics of temozolomide in malignant glioma patients. *Clin Cancer Res* 10: 3728-3736, 2004.
30. Patel M, McCully C, Godwin K and Balis FM: Plasma and cerebrospinal fluid pharmacokinetics of intravenous temozolomide in non-human primates. *J Neurooncol* 61: 203-207, 2003.
31. Cimmino G, Pepe S, Laus G, Chianese M, Prece D, Penitente R and Quesada P: Poly(ADP-ribose) polymerase-1 signalling of the DNA damage induced by DNA topoisomerase I poison in D54(p53wt) and U251(p53mut) glioblastoma cell lines. *Pharmacol Res* 55: 49-56, 2007.
32. Sabisz M, Wesierska-Gadek J and Skladanowski A: Increased cytotoxicity of an unusual DNA topoisomerase II inhibitor compound C-1305 toward HeLa cells with downregulated PARP-1 activity results from re-activation of the p53 pathway and modulation of mitotic checkpoints. *Biochem Pharmacol* 79: 1387-1397, 2010.
33. Zhang J, Stevens MF, Laughton CA, Madhusudan S and Bradshaw TD: Acquired resistance to temozolomide in glioma cell lines: Molecular mechanisms and potential translational applications. *Oncology* 78: 103-114, 2010.
34. Cieřlar-Pobuda A, Saenko Y and Rzeszowska-Wolny J: PARP-1 inhibition induces a late increase in the level of reactive oxygen species in cells after ionizing radiation. *Mutat Res* 732: 9-15, 2012.
35. Sabbatino F, Fusciello C, Somma D, Pacelli R, Poudel R, Pepin D, Leonardi A, Carlomagno C, Della Vittoria Scarpati G, Ferrone S and Pepe S: Effect of p53 activity on the sensitivity of human glioblastoma cells to PARP-1 inhibitor in combination with topoisomerase I inhibitor or radiation. *Cytometry A* 85: 953-961, 2014.
36. Franken NA, Rodermond HM, Stap J, Haveman J and van Bree C: Clonogenic assay of cells in vitro. *Nat Protoc* 1: 2315-2319, 2006.
37. Livak KJ and Schmittgen TD: Analysis of relative gene expression data using real-time quantitative PCR and the 2(-Delta Delta C(T)) method. *Methods* 25: 402-408, 2001.
38. Atkins RJ, Ng W, Stylli SS, Hovens CM and Kaye AH: Repair mechanisms help glioblastoma resist treatment. *J Clin Neurosci* 22: 14-20, 2015.
39. Sandhu SK, Yap TA and de Bono JS: Poly(ADP-ribose) polymerase inhibitors in cancer treatment: A clinical perspective. *Eur J Cancer* 46: 9-20, 2010.
40. Majuelos-Melguizo J, Rodríguez MI, López-Jiménez L, Rodríguez-Vargas JM, Martí Martín-Consuegra JM, Serrano-Sáenz S, Gavard J, de Almodóvar JM and Oliver FJ: PARP targeting counteracts gliomagenesis through induction of mitotic catastrophe and aggravation of deficiency in homologous recombination in PTEN-mutant glioma. *Oncotarget* 6: 4790-4803, 2015.
41. Tentori L, Ricci-Vitiani L, Muzi A, Ciccarone F, Pelacchi F, Calabrese R, Runci D, Pallini R, Caiafa P and Graziani G: Pharmacological inhibition of poly(ADP-ribose) polymerase-1 modulates resistance of human glioblastoma stem cells to temozolomide. *BMC Cancer* 14: 151, 2014.
42. Erice O, Smith MP, White R, Goicoechea I, Barriuso J, Jones C, Margison GP, Acosta JC, Wellbrock C and Arozarena I: MGMT expression predicts PARP-mediated resistance to temozolomide. *Mol Cancer Ther* 14: 1236-1246, 2015.
43. Gupta A, Yang Q, Pandita RK, Hunt CR, Xiang T, Misri S, Zeng S, Pagan J, Jeffery J, Puc J, *et al*: Cell cycle checkpoint defects contribute to genomic instability in PTEN deficient cells independent of DNA DSB repair. *Cell Cycle* 8: 2198-2210, 2009.
44. Balvers RK, Lamfers ML, Kloezezan JJ, Kleijn A, Berghauer Pont LM, Dirven CM and Leenstra S: ABT-888 enhances cytotoxic effects of temozolomide independent of MGMT status in serum free cultured glioma cells. *J Transl Med* 13: 74, 2015.
45. Godoy PR, Mello SS, Magalhães DA, Donaires FS, Nicolucci P, Donadi EA, Passos GA and Sakamoto-Hojo ET: Ionizing radiation-induced gene expression changes in TP53 proficient and deficient glioblastoma cell lines. *Mutat Res* 756: 46-55, 2013.
46. Zaky A, Busso C, Izumi T, Chattopadhyay R, Bassiouny A, Mitra S and Bhakat KK: Regulation of the human AP-endonuclease (APE1/Ref-1) expression by the tumor suppressor p53 in response to DNA damage. *Nucleic Acids Res* 36: 1555-1566, 2008.
47. Poletto M, Legrand AJ, Fletcher SC and Dianov GL: P53 coordinates base excision repair to prevent genomic instability. *Nucleic Acids Res* 44: 3165-3175, 2016.
48. Ströbel T, Madlener S, Tuna S, Vose S, Lagerweij T, Wurdinger T, Vierlinger K, Wöhrer A, Price BD, Dimple B, *et al*: Ape1 guides DNA repair pathway choice that is associated with drug tolerance in glioblastoma. *Sci Rep* 7: 9674, 2017.
49. Ming M and He YY: PTEN in DNA damage repair. *Cancer Lett* 319: 125-129, 2012.
50. Mukherjee A and Karmakar P: Attenuation of PTEN perturbs genomic stability via activation of Akt and down-regulation of Rad51 in human embryonic kidney cells. *Mol Carcinog* 52: 611-618, 2013.
51. Hunt CR, Gupta A, Horikoshi N and Pandita TK: Does PTEN loss impair DNA double-strand break repair by homologous recombination? *Clin Cancer Res* 18: 920-922, 2012.
52. Fu D, Calvo JA and Samson LD: Balancing repair and tolerance of DNA damage caused by alkylating agents. *Nat Rev Cancer* 12: 104-120, 2012.
53. Schuhwerk H, Atteya R, Siniuk K and Wang ZQ: PARPping for balance in the homeostasis of poly(ADP-ribosylation). *Semin Cell Dev Biol* 63: 81-91, 2017.

54. Chai KM, Wang CY, Liaw HJ, Fang KM, Yang CS and Tzeng SF: Downregulation of BRCA1-BRCA2-containing complex subunit 3 sensitizes glioma cells to temozolomide. *Oncotarget* 5: 10901-10915, 2014.
55. Ray Chaudhuri A and Nussenzweig A: The multifaceted roles of PARP1 in DNA repair and chromatin remodelling (Review). *Nat Rev Mol Cell Biol* 18: 610-621, 2017.
56. Polo SE and Jackson SP: Dynamics of DNA damage response proteins at DNA breaks: A focus on protein modifications. *Genes Dev* 25: 409-433, 2011.
57. Nagel ZD, Kitange GJ, Gupta SK, Joughin BA, Chaim IA, Mazzucato P, Lauffenburger DA, Sarkaria JN and Samson LD: DNA repair capacity in multiple pathways predicts chemoresistance in glioblastoma multiforme. *Cancer Res* 77: 198-206, 2017.